Biointerface Research in Applied Chemistry
Open-Access Journal (ISSN: 2069-5837)

Article
Volume 13, Issue 4, 2023, 371
https://doi.org/10.33263/BRIAC134.371

Ligand and Structure-Based Pharmacophore Modelling, Computer-aided Screening and Molecular Docking to Detect Novel NS5B Polymerase Inhibitors as Anti-HCV Compounds

Anuradha Derashri [1], Akanksha Dwivedi [2], Monika Maan [3], Divya Dhawal Bhandari [4,*]

[1] Gahlot Institute of Pharmacy, Navi Mumbai, Maharashtra 400709, anuradhaderashri@gmail.com (A.D.);
[2] Acropolis Institute of Pharmaceutical Education and Research, Indore, M. P. 453771; akd.pharma@gmail.com (A.D.);
[3] LBS College of Pharmacy, Jaipur, Rajasthan 303122; monikamaan12@gmail.com (M.M.);
[4] University Institute of Pharma Sciences, Chandigarh University, Mohali, Punjab, 140413; nainagumber@gmail.com (D.B.);
* Correspondence: nainagumber@gmail.com (D.B.);

Scopus Author ID 57218531605
Received: 29.04.2022; Accepted: 3.06.2022; Published: 7.10.2022

Abstract: The ongoing interest of researchers in the direct-acting NS5B inhibitors in the development of viral disease hepatitis has attracted our attention in the direction of the development of a quantitative four-featured pharmacophore model containing HBA (2), HY (1), and PI (1) features. The model showed correlation coefficient, RMSD, and cost difference values as 0.895, 0.911, and 30.896, respectively. The model validation is done by using Fisher's randomization test (99%), internal and external tests set the expectation with r2 values of 0.80 and 0.65. Simultaneously, the 3D crystal structure of NS5B was utilized for generating a pharmacophore model design based on a structure with features generation 2 Hydrogen Bond Acceptors, 2 Hydrogen Bond Donors, and 2 Hydrophilic features. Further on these two models, HITS searches using NCI and Maybridge databases were done. Three hundred forty-five compounds were screened, and the three greatest potent hits were docked to the active site of NS5B. It was found that these docked conformations showed interactions with GLN446 and TYR448 amino acids, which are located at NS5B active site. In an instant, with the use of various computational methods in a sequence, we have identified novel structurally diverse NS5B inhibitors.

Keywords: Hepatitis C virus; pharmacophore; virtual screening; docking, NCI; Maybridge.

1. Introduction

Over the past few decades, we have observed several global viral infection outbreaks, one of which is chronic hepatitis C; worldwide, an estimated 58 million people have about 1.5 million new infections occurring annually. It is said by who reported in 2019 that approximately 290'000 people died from hepatitis C, mostly from cirrhosis and hepatocellular carcinoma (1° liver cancer). Enduring HCV infections can lead to liver and hepatocellular carcinoma, being the largest cause of liver transplants and ultimately causing a financial burden on the healthcare system. Flaviviridae is the family of this virus, which comprises the Flavivirus and Pestivirus genera [1], which are responsible for human and cattle ailments.

Hepatitis C virus((+)-ssRNA) is around 9.6kb in length, having a diameter of 40–60 nm. Genetically [1–6] are major genotypes with 31-34 percent nucleotide differences. HCV

genotype has 3000 amino acids on a single polyprotein chain. Viral and cellular proteases involved in the proteolytic processing of this polyprotein chain are responsible for the formation of two parts, i.e., structural proteins (core, E1, E2, and p7) and non-structural proteins (NS2, NS3, NS4A, NS4B, NS5A, and NS5B) [2]. Currently, no effective medication and vaccine is available for HCV due to strain disparity, a wide range of genotypes, and their mode of action. The existing treatment, consisting of a blend of pegylated interferon-alfa and the nucleoside analog ribavirin, is accompanied by serious health issues such as fatigue, hemolytic anemia, depression, and flu-like symptoms, all of which lead to medication non-adherence. These symptoms challenge identifying novel, safe and effective therapeutics for their prevention and treatment. Because NS5B polymerase is a key protein for viral replication, it's the best target for intense research [3]. Structurally NS5B polymerase has a 3D rightward profile, i.e., finger, palm, and thumb. The palm subdomain contains the NS5B polymerase active site and three aspartic acids (Asp318, Asp319, and Asp220) that coordinate two Mg^{2+} ions throughout the polymerization response and lead to improved efficacy and tolerability [4].

Non-structural protein 5B (NS5B) inhibitors may be characterized into three classes—nucleoside active site inhibitors (NIs), non-nucleoside allosteric inhibitors (NNIs), and pyrophosphate analogs, subsequently, classified into several classes resulting in inhibition of viral RNA replication at different stages and sites. Nucleoside inhibitors (Nis) of hepatitis C virus NS5B are divided into three major classes: purine nucleoside inhibitors, pyrimidine nucleoside inhibitors, and miscellaneous nucleoside inhibitors. They are also known as chain-terminating inhibitors because they stop RNA synthesis and perform chain termination by preventing incoming nucleotides from being added to the RNA chain. It has been anticipated that steric hindrance at the catalytic location of NS5B, which contains a 3’-hydroxyl group, blocks the polymerase catalytic activity resulting in chain termination.

Non-nucleoside inhibitors(NNIs) are classified into three distinct types: active site inhibitors, allosteric site inhibitors, and miscellaneous NNIs. Active site inhibitors neither compete with nucleotides nor the RNA template. Instead, they inhibit polymerase activity by inhibiting conformational changes by binding to RNA-dependent RNA polymerase, known for required NS5B activity. The second category of NNI aims at the allosteric sites of NS5B, causing conformational deviations and consequently lowering or obstructing enzyme activity. For other non-nucleoside analog inhibitors, the binding site is either not defined or under further investigation [5].

Molecular modeling has been growing as an important promising tool for drug discovery for the past few years. The advantages include an accelerated lead identification process, as well as. Thus, *in-silico* data gives information about the ligand-protein interaction. Thus molecular modeling is of utmost importance along with pharmacodynamic applications to determine lead compounds' pharmacokinetic fate.

Various new methods available these days differ from each other based on response data by the computer and application scale [6]. After the fruitful results obtained via computational drug designing to identify the lead compound, we envisioned identifying new, architecturally differing non-nucleoside Hcv NS5B inhibitors using a model-based virtual screening and molecular docking approach.

2. Materials and Methods

2.1. Ligand-based 3-D pharmacophore generation.

In light of high structural variation in biological activity (0.005 to 17.0µm), a series of 54 NS5B polymerase inhibitors were chosen from the literature. The chemical structures were drawn of all the compounds using Chem. Draw 8.0 and export to Discovery Studio (DS). The energy of all the compounds was minimized, and conformational analysis was carried out. A maximum of 255 conformations for each compound were generated using the CHARM Force field-based best conformation model generation method. All the molecules under consideration were divided into two groups: a training set of 35 compounds and a test set of 19 compounds. Utmost attention was taken to confirm ample diversity in both sets [7].

2.2 Pharmacophore modeling.

Since selecting the chemical features is the most important step in pharmacophore generation, the common chemical feature mapping module of DS was employed to identify the common features among the compounds. Instead of identifying the superlative 3-dimensional arrangement of chemical features by using only the bottom energy conformation of each compound and in each training set, all conformational models were used.

During the common features hypothesis generation process, four features appeared to be shared by all of the training set compounds: two hydrogen bond acceptor-lipid HBA (LI) features, one hydrophobic (HY) feature, and one positive ionizable (PI) feature. As a result, these prominent features were used to generate quantifiable pharmacophore hypotheses with an uncertainty value of 3 and MinPoints and MinSubset Points values of 4. The MinPoints parameter determines the minimum number of location constraints required for any hypothesis. The MinSubset Point parameter specifies the minimum requirement of chemical features a hypothesis must match in all the data sets of compounds [8].

In hypothesis generation, the "Hypogen algorithm", is used to calculate three main cost parameters (fixed cost, null cost, and total cost) in the unit of bits. "Fixed cost" is the lowest possible value representing a model that perfectly fits all data. "Null cost" is the highest value that assumes no relationship exists in the data and those experimental activities are normally distributed around their mean. The term "total cost" refers to three cost parameters: weight, configuration, and error. The value of weight cost rises if the model's feature weight deviates from an ideal value of 2. The error cost represents the difference between the estimated activities of the training set and their experimentally determined values, and the configuration cost represents the hypothesis's complexity [9]. For a significant pharmacophore model, the configuration value should not exceed a maximum of 17. It is always preferable if the difference between the null cost and the total cost is greater than 20 bits and the total cost value is close to the fixed cost value. If the value of RMS is low, it shows that the correlation between the estimated and the actual activity data is good, which further supports the predictive ability of the generated pharmacophore models. Among various available pharmacophore hypotheses, the one with low RMS value, high correlation coefficient (r), and the high difference between null and total cost was considered the best hypothesis and was further subjected to rigorous validation using cat scramble, internal test set, external test set and clinical drug candidate prediction [10].

2.3. Cat scramble validation.

To assess the statistical significance of the pharmacophore hypotheses generated from the training set molecules, Cat Scramble validation was performed. Fischer's randomization test serves as the foundation for this validation technique. The reason behind the analysis was to validate the strong relationship between chemical structures and biological activity. In this test, the activity values of the training set molecules are reassigned by randomization using the Cat Scramble technique, and new spreadsheets are created. The number of spreadsheets required is determined by the level of statistical significance desired. For 98 % and 99 % confidence levels, 49 and 99 spreadsheets are created, and 19 spreadsheets for 95% confidence levels, respectively. During the course of the study, a confidence level of 99 percent was chosen, and 99 spreadsheets were created. These spreadsheets were used to generate hypotheses with the same features and parameters as the original pharmacophore hypotheses, and the results were analyzed [11].

2.4. Internal test set prediction.

A common method of validation is the ability of the models to forecast biological activity for compounds outside of the model development. To assess the statistical significance of the developed model, an internal test set of 19 compounds was used. All the compounds in the internal test set were mapped onto the generated pharmacophoric model and predicted activities, and fit values were observed. The fit function considers not only the feature mapping but also the distance term, which measures the distance between the feature on the molecule and the centroid of the hypothesis feature [12].

2.5. External test set prediction.

The created pharmacophore was also authenticated by using an external set of structurally diverse NS5B inhibitors. The actual activity of these compounds ranged from 0.0008 to 0.55. The selected nine external test set compounds were mapped on the built pharmacophore model, and the results were analyzed [13].

In order to further confirm the universality and predictive ability of the developed model, some marketed drugs were mapped onto the chosen pharmacophore & their estimated and fit values were observed.

2.6. Virtual screening of chemical compound database.

A validated pharmacophore model with two HBA (LI), one HY, and one PI feature was used as a query to search the chemical compound databases viz Maybridge and NCI, which contained three lac thirty thousand two hundred forty compounds. Fit value, estimated value, and Lipinski's rule of five were employed to separate the retrieved hits [14].

2.7. Structure-based 3D pharmacophore generation.

A structure-based pharmacophore is a powerful tool for rapidly identifying structural requirements for effective ligand-receptor binding. The structure-based pharmacophore model can interpret intermolecular interactions amid proteins and their ligands. As soon as the pharmacophore model is identified, it can be employed as a prevailing means for the innovation and development of novel hits.

The 3D structure of HCV-NS5B rd-rp complexed with PHA-00729145 (PDB entry 1VYF) has been used for structure-based pharmacophore generation. The protein structure was checked for valence and missing hydrogen before being checked for any structural errors using the protein health check tool. Active site identification was then performed on the cleaned enzyme structure [15]. The active receptor site was identified using a sphere with a radius and location adjusted to 9.0 A° to include the active site and the key residues of the protein involved in ligand interaction. The interaction maps were generated with the density of lipophilic sites and density of polar sites parameters set to 10. In particular, functional features such as hydrogen bond acceptors, donors, and lipophilic groups were recognized in the dynamic position, and complementary features were placed within the binding position in a chemically rational site. Following a numeral of recapitulations, the concluding hypothesis was selected, which included six features: two hydrogen bond donors, two hydrogen bond acceptors, and two hydrophobic groups (with an additional 10 excluded volumes) describing the interactions amid the protein and ligand [16].

The structure-guided pharmacophore was authenticated by plotting Ana-setrubuvir, PI6130, NM283, Balapiravim, and IDX184, which are acknowledged as NS5B polymerase inhibitors.

2.8. Virtual screening of a chemical compound database.

Similar to ligand-driven pharmacophore-based virtual screening, the established structure-based pharmacophore was employed to separate NCI and Maybridge databases. The organization of the retrieved hits was done based on fit values, estimated values, and Lipinski's rule of five [17].

2.9. Validation of identified hits by cross-application of ligand-based and structure-based pharmacophores.

2.9.1 Pharmacophore mapping.

The NCI and Maybridge hits obtained from a ligand-based virtual screening protocol were mapped onto the structure-driven pharmacophore, and NCI hits obtained from a structure-based virtual screening protocol were mapped onto the ligand-based pharmacophore. The mapping patterns of all the hits, along with fit values, were analyzed [18]**.**

2.9.2 Molecular docking.

The ability of ligand-based and structure-based pharmacophore hits to interrelate with NS5B active site amino acids was explored. The experimental studies related to molecular docking were carried out with the help of the Libdocker program. This molecular dynamic simulated annealing-based algorithm is available as an extension of DS V.2.0 [19]. As described in the previous section, the complex crystal structure of NS5B RNA-dependent RNA polymerase was prepared. The protein was defined as the receptor molecule, and the crystal ligand was used to define the 9 Angstrom binding site on the receptor molecule. All of the hits and known NS5B inhibitors (Ana-setrobuvir, PI-6130, NM283, IDX-184, and Balapiravim) had their structures docked into the active position. In conclusion, all the probable interaction means for various configurations were scrutinized based on Libdocker interaction dynamisms [20].

3. Results and Discussion

3.1. Ligand built 3D pharmacophore generation.

A pharmacophore model was created using 35 compounds in the training set representing a sequence of structurally distinct compounds Figure 1.

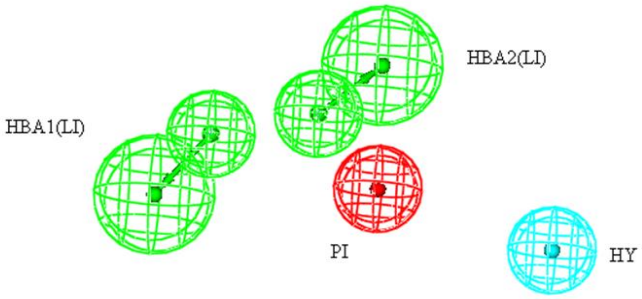

Figure 1. Ligand-based pharmacophore model.

Out of various generated models, a set of 10 hypotheses was chosen**.** Their cost values, correlation coefficients (*r*), RMS deviations, and pharmacophore features are listed in Table 1.

Table 1. Performance of top ten pharmacophoric hypotheses generated.

Hypo. no	Total cost	Correlation(r)	RMS	Configuration	Features
1	154.245	0.89	0.91	16.79	2HBALi,1HY,1PI
2	159.697	0.81	1.14	16.79	2HBALi,1HY,1PI
3	160.56	0.80	1.16	16.79	2HBALi,1HY,1PI
4	161.67	0.79	1.20	16.79	2HBALi,1HY,1PI
5	161.97	0.79	1.19	16.79	2HBALi,1HY,1PI
6	162.38	0.80	1.18	16.79	2HBALi,1HY,1PI
7	162.54	0.78	1.22	16.79	2HBALi,1HY,1PI
8	162.97	0.79	1.21	16.79	2HBALi,1HY,1PI
9	163.45	0.77	1.24	16.79	2HBALi,1HY,1PI
10	163.83	0.78	1.23	16.79	2HBALi,1HY,1PI

The total cost of each hypothesis was discovered to be close to the fixed cost values, which is thought to be significant for a good model.

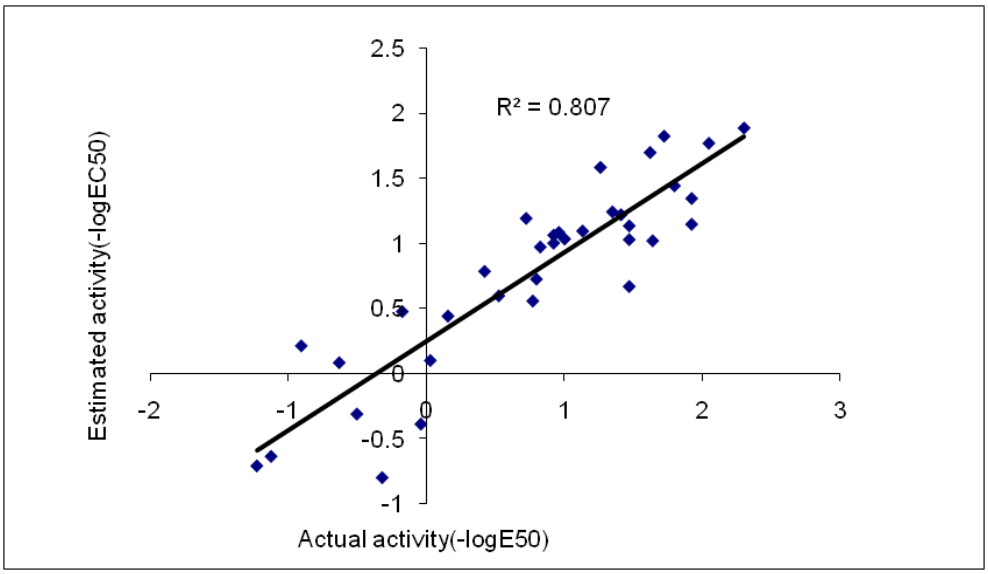

Figure 2. A plot of actual versus estimated activities of compounds from the training set.

The hypotheses' configuration cost value was 16.79, which was within the acceptable limit. Hypothesis 1, which consisted of two HBA (LI), one HY, and one positive ionizable feature, had the highest cost difference (30.89 bits), the lowest error cost (132.28), the lowest rms difference (0.91), and the best correlation coefficient (0.89) [21]. Figure 2 depicts a plot of actual versus estimated activities of compounds from the training set.

While mapping training set compounds onto chosen pharmacophore, it was observed that the most active compound (actual activity=0. 005, estimated value=0.013) mapped perfectly onto the generated model with a fit value of 10.766. HBA 1 feature mapped over oxygen of methyl sulphonyl methane, HBA 2 mapped over oxygen of sulphonyl group of pyrimidine ring, PI feature mapped onto the pyrimidine ring, and HY mapped onto 2-pentyl pyridazine-3(2H)–one. Mapping of least active molecule (actual activity=17, estimated value=5.046) exhibited a fit value of 8.167 with only three feature mapping; HBA 1 mapped over oxygen of sulphonyl group, HBA 2 could not map any of the functional group, PI mapped onto nitrogen of pyrimidine ring, HY mapped onto pentyl pyridazine-3(2*H*) –one. The mapping pattern of most and least active compounds clearly shows that the model has the ability to discriminate between actives and inactives, which is always desirable for a good pharmacophore model [22]. Figure 3 depicts the mapping of the most active (A) and least active (B) compound onto the developed pharmacophore.

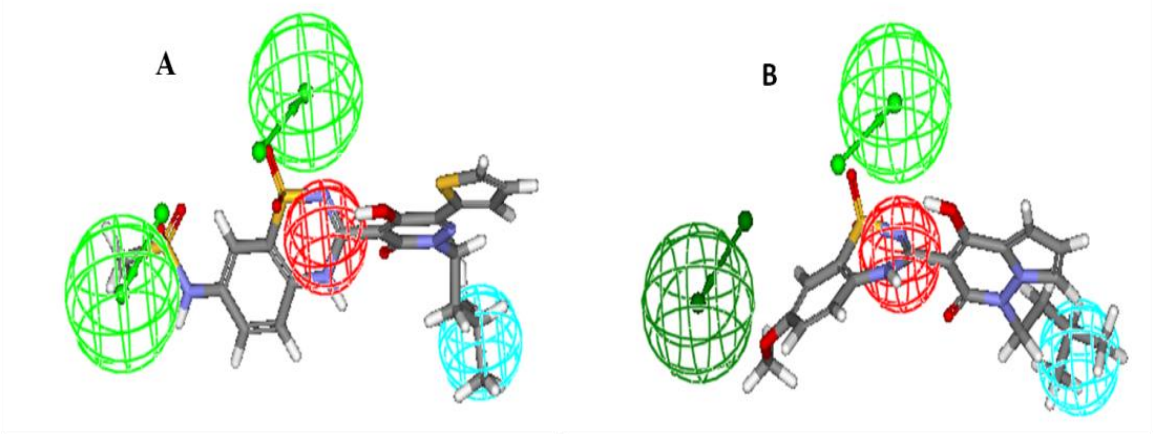

Figure 3 Mapping of **(A)** the most active and **(B)** least active compound onto ligand-based pharmacophore model.

Since the chosen pharmacophore model showed all signs of statistical fitness, it was subjected to rigorous validation to ensure further the model's accuracy, universality, and predictability.

3.2. Cat scramble validation.

The pharmacophore's quality was evaluated using the Fischer validation method at a confidence level of 99 percent. The experimental activities in the training set were randomly scrambled using the Cat Scramble program, and the resulting training set was used for the HypoGen run. Out of 99 trials, all had a correlation value of less than 0.90, with very high RMS deviation and total cost (Figure 4). In conclusion, none of the generated hypotheses outperformed the original hypothesis in terms of statistics, and the results of the cat scramble provided high confidence in hypothesis 1 [23].

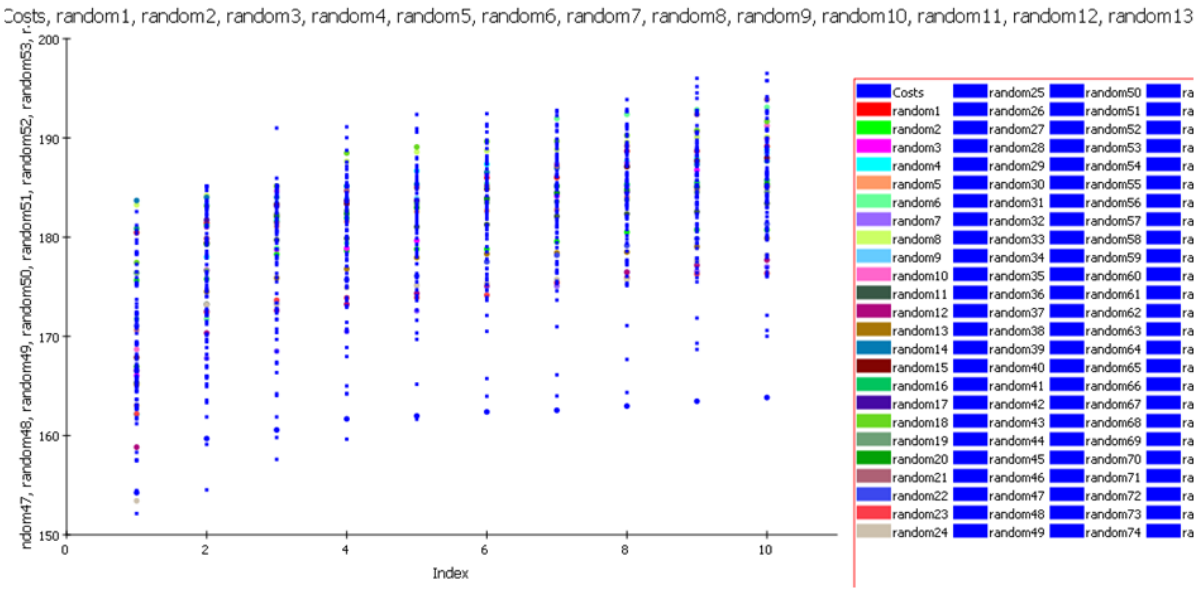

Figure 4. Fisher validation cost data (99%).

3.3. Internal test set validation.

Using the developed model, a test set consisting of 19 compounds was subjected to pharmacophore mapping analysis. A correlation coefficient of 0.70 (Figure 5) indicated a good correlation between the actual and estimated activities. The internal test set prediction results revealed the model's high statistical fitness and predictability [24]. Figure 4 shows a plot between actual versus estimated activities of the test set compound.

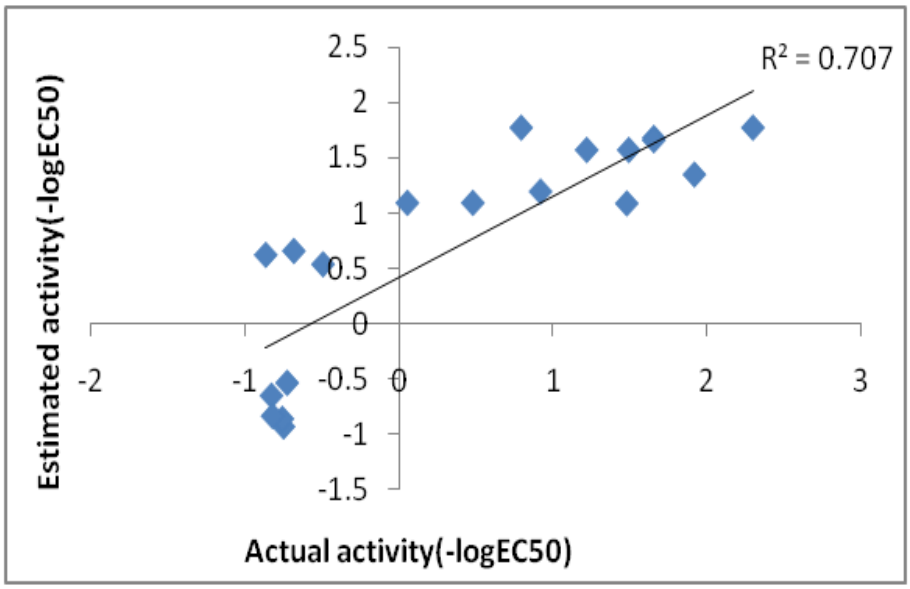

Figure 5. A plot of actual versus estimated activity of test set compounds

3.4. External test set validation.

An external test set comprising ten structurally diverse compounds was used to validate the pharmacophore model further. The structure of all the test set compounds was mapped onto the chosen pharmacophore model, and a squared Correlation coefficient value of 0.65 between actual and estimated values indicated the good predictive capability of the pharmacophore model. As expected, the most active compound (3A) exhibited good mapping with a fit value of 8.024. The results of the external test set prediction firmly established the predictivity of the

pharmacophore model. Figure 6 shows a plot of the actual versus estimated activity of the external test set compound.

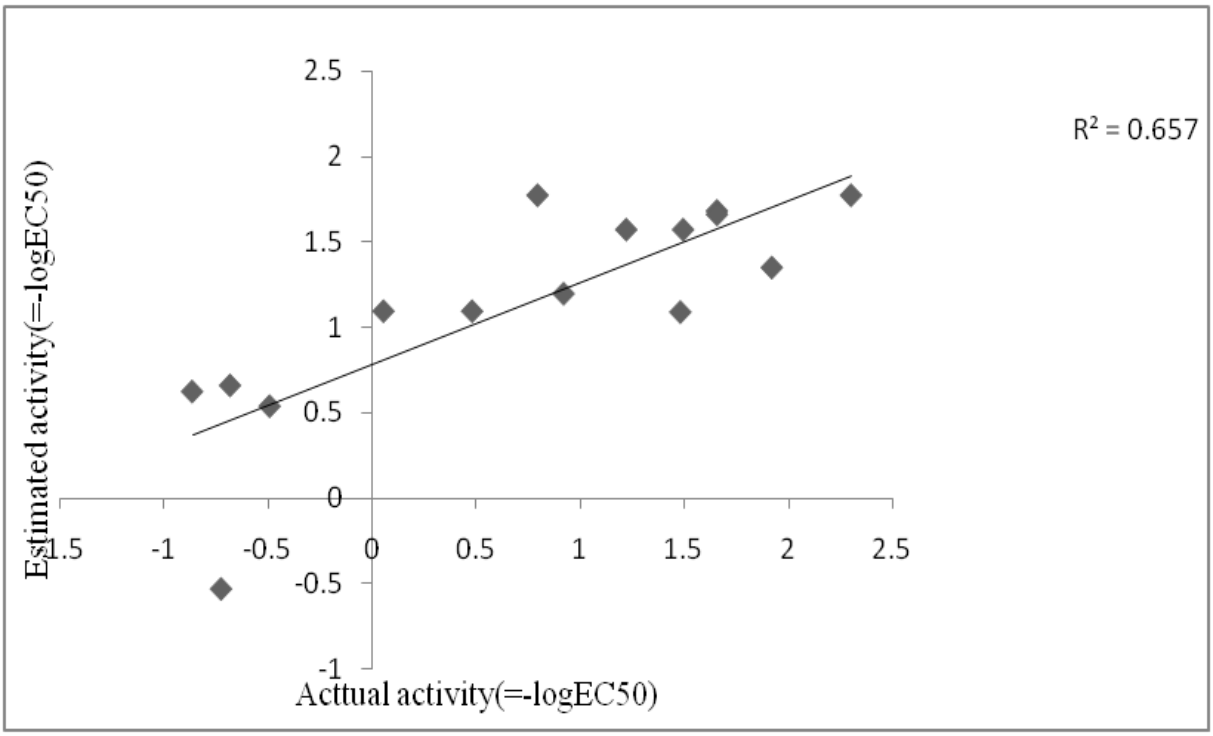

Figure 6. A plot of actual versus estimated activity of external test set compounds.

Finally, the generated pharmacophore was validated by mapping marketed drugs, namely, Ana-setrubuvir, PI6130, NM283, Balapiravim, IDX184. All the drugs showed three features mapping with fit values 7.384, 6.420, 6.277, 6.525, and 7.243, respectively. The fit values and feature mapping pattern confirmed the soundness and universality of the model [25].

3.5. Ligand-driven pharmacophore-based virtual screening.

The thoroughly validated pharmacophore model was used as a query for retrieving compounds from NCI and MayBridge chemical compound database. As a result, 299 and 46 hits were retrieved from NCI and Maybridge databases, respectively. The retrieved hits were filtered based on fit value, estimated value, and Lipinski's rule of five [26].

Finally, 10 compounds namely NSC14659, NSC29644, NSC4356, NSC18503, NSC414, GK03124, AW00783, AW00785, KM08645, CD11501 turned out to be potential ligands exhibiting a perfect full feature mapping with good fit values of 9.631,9.52,9.509,9.221, 8.835,9.212,8.466,8.322,8.013 and7.931, high estimated value of 0.17 ,0.22 ,0.23 ,0.44,1.0,0.45,2.53,3.52,7.19,8.68µm respectively and zero Lipinski's violation. Out of 10 hits, the two most compounds (NSC14659 and GK03124) showed the highest predicted activity of 0.17 µm and 0.45 µm.

In the case of NSC14659, HBA 1 feature mapped well onto the oxygen of ethane 1, 2 -diol, and HBA 2 was occupied by another oxygen of ethane 1, 2 -diol, while the hydrophobic (HY 1) feature mapped onto the 2 methoxybuta-1-3-diene presents on either side of the benzene ring and positive ionizable (PI 1) feature mapped onto nitrogen of 3-ethylamino –propane -1-2-diol group.

Similarly, in the case of GK03124, HBA 1 was occupied by the sulfur of 4, 5-dimethyl-2-3-dihydrothiophene group, whereas HBA 2 was mapped well onto oxygen of methyl formate. Hydrophobe (HY1) mapped onto hydrogen of toluene and positive ionizable (PI1) mapped onto nitrogen of di-isopropyl amino ethyl. The suitability of NSC14659 and GK03124 was further evaluated by mapping both compounds onto the structure-based pharmacophore generated using the structure of NS5B Rd-Rp obtained from PDB (1VYF) [27]. The mapping of GK03124 and NSC14659onto ligand-based pharmacophore model is depicted in Figure 7.

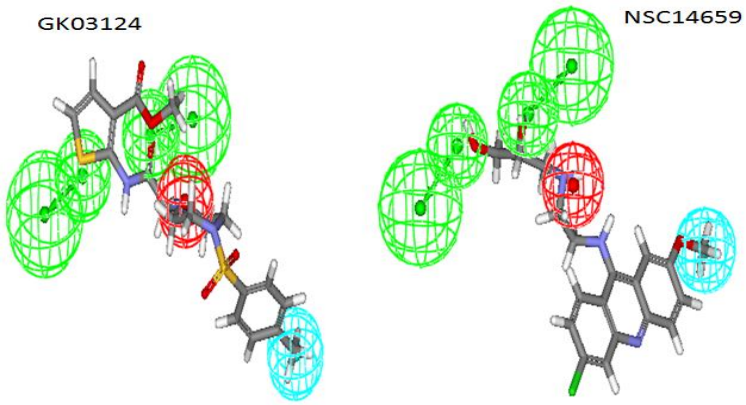

Figure 7 Mapping of NSC14659 and GK03124 onto ligand-based pharmacophore model.

3.6. Structure-based 3D pharmacophore generation.

The pharmacophore derived from the 3D structure of a protein (PDB code 1VYF) with six features: two hydrogen bond donors, two hydrogen bond acceptors, and two hydrophobic groups (Figure 8) were validated by mapping of Ana-setrobuvir Balapiravim, IDX184, NM283, and PI6130. The identified NS5B inhibitors exhibited four feature mapping with a decent fit value, demonstrating the model's precision and strength [28].

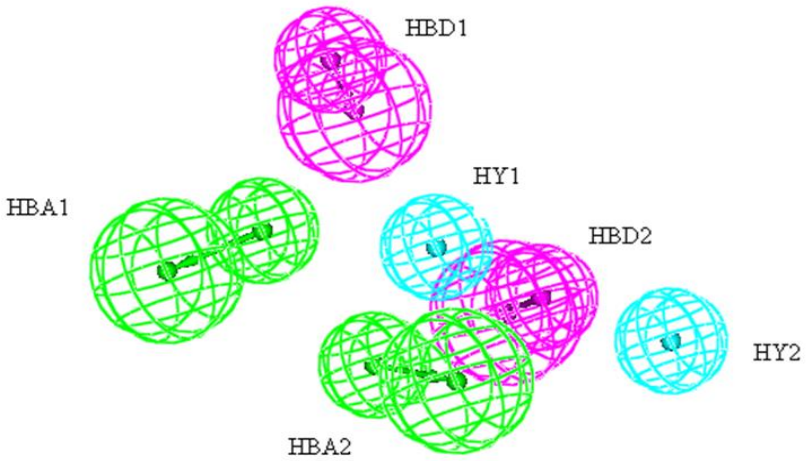

Figure 8 Structure-based pharmacophore model.

Comparing pharmacophoric features extracted from the structure-based and ligand-based pharmacophore revealed that both models share three common features: two hydrogen bond acceptors (HBA) and one hydrophobic group (HY2). Even the inter-feature distances (HBA1 to HBA2, HBA1 to HY1, HBA 2 to HY1) in the ligand-based pharmacophore model were nearly identical to those in the structure-based pharmacophore model (Table 2). The pharmacophore so achieved by using a structure-based study exhibited three additional features, namely two hydrogen bond donors (HBD1 and 2) and one hydrophobe (HY1),

whereas the pharmacophore obtained from the ligand-based study exhibited one additional feature, namely positive ionizability (PI) [29].

Table 2. Interfeature distances between ligand-based and structure-based pharmacophore features.

	Interfeature distance	
Pharmacophore features	**LBDD**	**SBDD**
HBA1-HBA2	9.48	10.65
HBA1-HY1	15.18	15.57
HBA2-HY1	13.17	13.30
HBA1-HY2	-	8.33
HBA2-HY2	-	8.65
HBA1-PI	8.113	-
HBA2-PI	4.487	-
HY1-PI	8.356	-

In order to recognize new, latent lead compounds, pharmacophore-based virtual screening was carried out using the NCI chemical compounds database. Two hundred forty-five hits were found and arranged based on their fit value and Lipinski's violation. Following categorization, five latent compounds were chosen: NSC353454, NSC250686, NSC250684, NSC109605, and NSC639365, with fit values ranging from 2.238 to 1.654 and no Lipinski's violation. NSC109605 exhibited full feature mapping and appeared to be the most active compound of the five (fit value 2.238).

3.7. Validation of identified hits.

3.7.1. Cross application of pharmacophores.

The NCI and Maybridge hits retrieved from ligand-driven pharmacophore-based virtual screening were mapped over the six featured pharmacophore models, and as expected, NSC14659, GK03124, showed a good fit value of 2.08, 1.94, and NSC 109605 when mapped on four feature ligand driven pharmacophore a fit value of 5.42 was observed [30].

3.7.2 Molecular docking studies.

With an aim to evaluate the precise molecular interaction of all three hits identified using ligand-based and structure-based pharmacophores, they were docked into the active site of HCV NS5B using Libdocker software implemented in DS. During the course of the study, it was perceived that the active site of the NS5B protein is surrounded by the ASP318, 319, ASN316, CYS366, GLN446, TYR 415, 448, MET414, ARG158, ASN411, SER556, ARG386, GLY449, ARG394SER446, 556, ASN291, amino acid residues (figure 9). NSC14659, GK03124, and NSC109605 showed good Libdocker interaction energy of 108.32, 118.35and 108.06, respectively [31]. The interaction analysis of the lead compound NSC14659 showed hydrogen bond interaction between oxygen present on 6-chloro-2-methoxyacridine with TYR415 and ARG158, hydrogen bond interaction with TYR448 and SER368 by -NH group, and hydrogen bond interaction with SER556, ASP318, and SER407 by CH_3OH group, and hydrogen bond interaction with ASP318, ASN291and GLN446 by –OH group. Methylamino propane-1, 2-diol exhibited hydrogen bond interaction with TYR195, ASN316, MET414, and CYS366. 6-chloro-2-methoxyacridine also showed Van der-Waals interaction with ARG158.

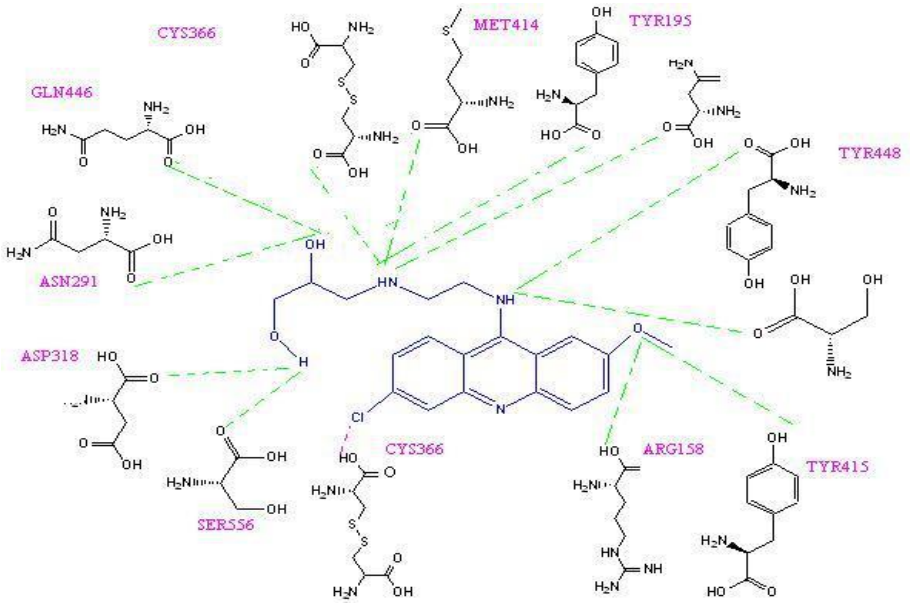

Figure 9. Molecular relationship of NSC14659 with active site amino acids.

Whereas the GK03124 showed hydrogen bond interaction between oxygen present on the 1-methyl-4-(methylsulphonyl) benzene with TYR415 and ASN291 (Figure 10), the same oxygen also showed Van der-Waals interaction with ASN291. Sulfur of 1 methyl-4-(methylsulphonyl) benzene ring showed hydrogen bond interaction with CYS366. Similarly, the oxygen of methyl thiophene-3-carboxylate exhibited hydrogen bond interaction with GLN446, ASN316, and SER556. Sulpher of 2-(methylamino) thiophene-3-carbaldehyde showed Van der-Waals interaction with GLY449, and its nitrogen showed Van der-Waals interaction with SER556. The hydrogen of decamethyl piperazine showed Van der-Waals interaction with TYR448 [32].

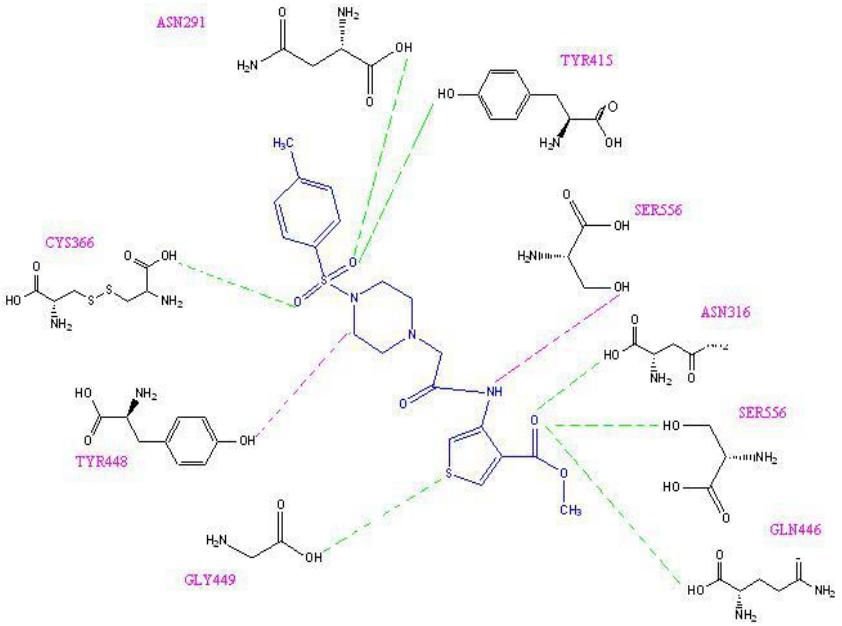

Figure 10. Molecular relationship of GK03124 with active site amino acids.

The NSC109605 hydroxyl group showed hydrogen bond interaction with MET414, CYS366, and ASP319 (Figure 11). On another side of the ring, the oxygen of ethanol exhibited hydrogen bond interaction with TYR448. The oxygen of benzaldehyde displayed hydrogen

bond interaction with TYR448, TYR415, and ASN316. The oxygen of anisole presented Van der-Waals interaction with ASN316 [33].

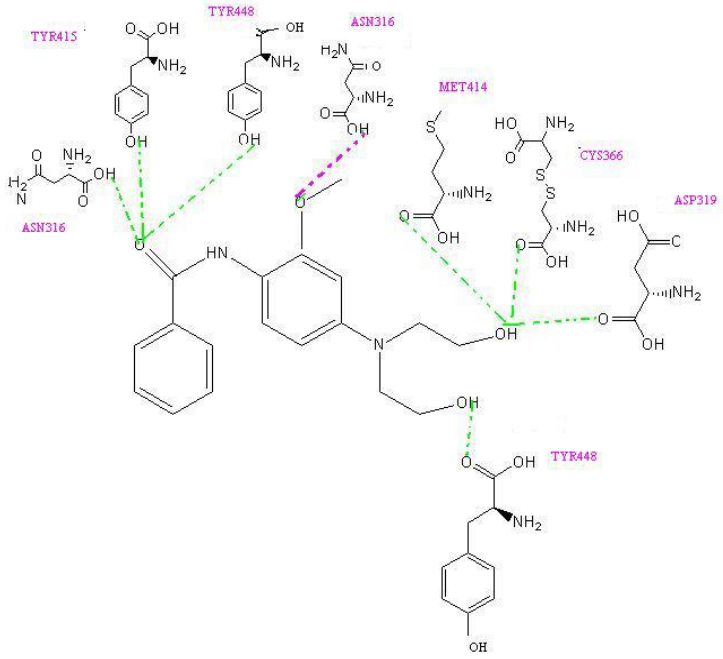

Figure 11. Molecular interaction of NSC109605 with active site amino acids.

As a reference known compound, NS5B inhibitor IDX-184 was also docked. Hydrogen bond interaction was observed between the nitrogen of 1-methyl-4, 5-dihydro-1H-imidazole, and TYR415. The nitrogen of 2 amino-5, 6-dihydropyrimidine 4(3-H)-one showed hydrogen bond interaction with the oxygen of SER556. Tetrahydrofuran-3,4diol showed hydrogen bond interaction with CYS366, ARG386, and ASN411 (Figure 12). The oxygen of dimethyl methyl phosphoramidite showed hydrogen bond interaction with CYS366 and GLY449, and its oxygen showed interaction with ASN316. N-methyl (phenyl) methanamine group exhibited hydrogen bond interaction with ASP318. The oxygen of the methanol group exhibited hydrogen bond interaction with GLN446 and also showed Van der-Waals interaction with GLN446 [34].

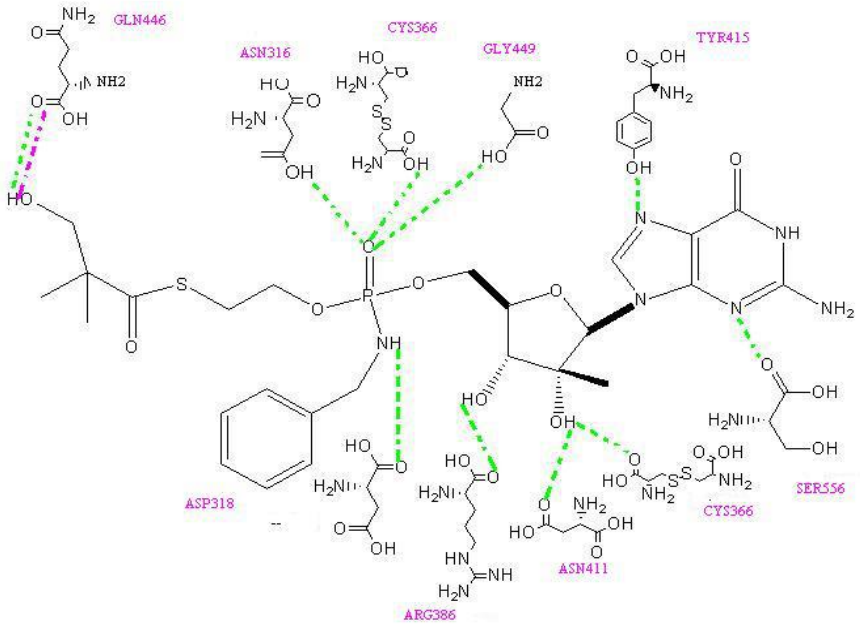

Figure 12. Molecular interaction of IDX184 with active site amino acids.

Reviews of previous literature have also revealed the importance of ASP318, 319, TYR 415,448, CYS366, GLN446, ARG158, and MET 414; in our study also, ASP318, 319, TYR 448, CYS366, MET 414, GLN446, and ARG158 has appeared as important amino acids. Since all three hits showed good interaction with important amino acid residues of the active site of NS5B polymerase, they hold good prospects for their future development into novel anti-HCV agents [35-36].

4. Conclusions

With the help of recent advances and the development of *in-silico* protocols, we have developed universal pharmacophores through structure and ligand-based molecular modeling. The thoroughly validated pharmacophore models have been used for database mining, leading to the retrieval of the three most potent and druggable NS5B inhibitors. The ability of all three hits (NSC14659, NSC109605, GK03124) to interact with NS5Bactive site amino acids has been evaluated using molecular docking studies, and the results revealed the importance of ASP318, 319, TYR 415,448, CYS366, GLN446, ARG158and MET 414 amino acids which are in agreement to previous studies. Current research has recognized three potent, structurally diverse, druggable, and novel NS5B inhibitors, which could be hoisted into anti-HCV drugs. In the future, NS5B inhibitors will likely form an integral part of more effective anti-HCV therapies.

Funding

This research received no external funding.

Acknowledgments

Banasthali University provided computational resources, and the authors thank Vice Chancellor Banasthali University for providing all the necessary facilities.

Conflicts of Interest

The authors declare no conflict of interest.

References

1. Deore, R.; Chern, J. NS5B RNA dependent RNA polymerase inhibitors: The promising approach to treat hepatitis C virus infections. *Current Medicinal Chemistry* **2010,** *17*, 3806-3826, https://doi.org/10.2174/092986710793205471.
2. Barreca, M. L.; Iraci, N.; Manfroni, G.; Cecchetti, V. Allosteric inhibition of the hepatitis C virus NS5B polymerase: *In sillico* strategies for drug discovery and development. *Future Medicinal Chemistry* **2011**, *3*, 1027-1055, https://doi.org/10.4155/fmc.11.53.
3. Furamen, A. P.; Lam, A. M.; Murakami, E. Nucleoside analog inhibitors of hepatitis C viral replication: Recent advances, challenges and trends. *Future Medicinal Chemistry* **2009**, *1*, 1429-1452, https://doi.org/10.4155/fmc.09.88.
4. Lange, C.; Sarrazin, C. Hepatitis C: New drugs. 4th edition. Flying Publisher, Germany, 239-261.
5. Chen, K. X.; Lesburg, A. C.; Yang, W. A novel class of highly potent irreversible hepatitis C virus NS5B polymerase inhibitors. *Journal of Medicinal Chemistry* **2012,** *55*, 2089-2101, https://doi.org/10.1021/jm201322r.
6. Das, D.; Hong, J.; Chen, S. H.; Wang, G. Recent advances in drug discovery of benzothiadiazine and related analogs as HCV NS5B polymerase inhibitors. *Bioorganic and Medicinal Chemistry* **2011**, *19*, 4690-4703, https://doi.org/10.1016/j.bmc.2011.06.079.

7. Accelrys Software Inc., Discovery Studio Visualizer, Release 3.5. Accelrys Software Inc., **2012**, San Diago.
8. Sekhar, C.; Vyas, K.; Nagesh, H. N.; Rao, V. S. Pharmacophore hypothesis for atypical antipsychotics. *Bulletin of the Korean Chemical* Society **2012**, *33***,** 2930-2936, https://doi.org/10.5012/bkcs.2012.33.9.2930.
9. Kansal, N.; Silakari, O.; Ravikumar, M. Three dimensional pharmacophore modeling for c-Kit receptor tyrosine kinase inhibitors. *European Journal of Medicinal Chemistry* **2012**, *45*, 393–404, https://doi.org/10.1016/j.ejmech.2009.09.013.
10. Lu, S. H.; Wu, J. W.; Liu, H. L.; Tsai, W. B.; Ho, Y. The discovery of potential acetylcholinesterase inhibitors: A combination of pharmacophore modelling, virtual screening, and molecular docking studies. *Journal of Biomedical Science* **2011**, *18*, 1-13, https://doi.org/10.1186/1423-0127-18-8.
11. Yadav, D.; Paliwal, S.; Yadav R, Pal M, Pandey A (2012) Identification of novel HIV 1- protease inhibitors: Application of ligand and structure based pharmacophore mapping and virtual screening. PLoS ONE 7: 48942, https://doi.org/10.1371/journal.pone.0048942.
12. Paliwal, S.; Pal, M.; Yadav, D.; Singh, S. Ligand based drug design studies using predictive pharmacophore model generation on 4H-1,2,4-triazoles as AT1 receptor antagonists. *Medicinal Chemistry Research* **2011**, *4*, 9756-9777, https://doi.org/10.1007/s00044-011-9756-4.
13. Acharya, B. N.; Kaushik, M. P. Pharmacophore-based predictive model generation for potent antimalarials targeting haem detoxification pathway. *Medicinal Chemistry Research* **2007**, *16*, 213–229, https://doi.org/10.1007/s00044-007-9025-8.
14. Nagarajan, S.; Ahmed, A.; Choo, H.; Cho, Y. S. 3D QSAR pharmacophore model based on diverse IKKβ inhibitors. *Journal of Molecular Modelling* **2011,** *17*, 209–218, https://link.springer.com/article/10.1007/s00894-010-0714-8.
15. Musmuca, I.; Caroli, A.; Mai, A. Combining 3-D quantitative structure-activity relationship with ligand based and structure based alignment procedures for *in* silico screening of new hepatitis C virus NS5B polymerase inhibitors. *Journal of Chemical Information and Modelling* **2010**, *50*, 662-676, https://doi.org/10.1007/s00894-010-0714-8.
16. Arooj, M.; Thangapandian, S.; John, S.; Hwang, S.; Park, J. K.; Lee, K. W. 3D QSAR pharmacophore modeling, in silico screening, and density functional theory (DFT) approaches for identification of human chymase inhibitors. *International Journal of Molecular Sciences* **2011**, *12*, 9236-9264. https://doi.org/10.3390/ijms12129236.
17. Suresh, N.; Vasanthi, N. S. Pharmacophore modeling and virtual screening studies to design potential protein tyrosine phosphatase 1B inhibitors as new leads. *Journal of Proteomics and Bioinformatics* **2010**, *3*, 20-28, http://citeseerx.ist.psu.edu/viewdoc/download?doi=10.1.1.634.4836&rep=rep1&type=pdf.do:10.4172/jpb.
18. Sakkiah, S.; Thangapandian, S.; John, S.; Kwon, Y. J.; Lee, K. W. 3D QSAR pharmacophore based virtual screening and molecular docking for identification of potential HSP 90 inhibitors. *European Journal of Medicinal Chemistry* **2010**, *45*, 2132–2140, https://doi.org/10.1016/j.ejmech.2010.01.016.
19. Chopra, M.; Gupta, R.; Gupta, S.; Saluja, D. Molecular modelling study on chemically diverse series of cyclooxygenase-2 selective inhibitors: generation of predictive pharmacophore model using catalyst. *Journal of Molecular Modelling* **2008**, *14*, 1087–1099, https://doi.org/10.1007/s00894-008-0350-8.
20. Kroemer, R.T. Structure-based drug design: Docking and scoring. *Current Protein and Peptide Science* **2007**, *8*, 312-328, https://doi.org/10.2174/138920307781369382.
21. Elghoneimy, L. K.; Ismail, M. I.; Boeckler, F. M.; Azzazy, H. M. E.; Ibrahim, T. M. Facilitating SARS CoV-2 RNA-Dependent RNA polymerase (RdRp) drug discovery by the aid of HCV NS5B palm subdomain binders: In silico approaches and benchmarking. *Computers in Biology and Medicine* **2011**, *134*, 1044-1068, https://doi.org/10.1016/j.compbiomed.2021.104468.
22. Veronika, T.; Zsofia, K. Structure-based molecular modelling in SAR analysis and lead optimization. *Computational and Structural Biotechnology Journal* **2021**, *19*, 1431-1444, https://doi.org/10.1016/j.csbj.2021.02.018.
23. Salimeh M., Razieh G., Farzin H., Amirhossein S. 3D-QSAR-Based Pharmacophore Modeling, Virtual Screening, and Molecular Docking Studies for Identification of Tubulin Inhibitors with Potential Anticancer Activity. *BioMedical Research International* **2021**, 1-20, https://doi.org/10.1155/2021/6480804.
24. Cai, C.; Wu, Q.; Hong, H.; He, L.; Liu, Z.; Gu, Y. et al. *In silico* identification of natural products from Traditional Chinese Medicine for cancer immunotherapy. *Scientific Reports* **2021**, *11*, 3332, https://doi.org/10.1038/s41598-021-82857-2.

25. Chen, Y.; Mathai, N.; Kirchmair, J. Scope of 3D shape-based approaches in predicting the macromolecular targets of structurally complex small molecules including natural products and macrocyclic ligands. *Journal of Chemical Information and Modelling* **2020**, *60*, 2858–2875, https://doi.org/10.1021/acs.jcim.0c00161.
26. Coimbra, J. R. M.; Baptista, S. J.; Dinis, T. C. P.; Silva, M. M. C.; Moreira, P. I.; Santos, A. E. Combining virtual screening protocol and in vitro evaluation towards the discovery of BACE1 inhibitors. *Biomolecules* **2020**, *10*, 535-557, https://doi.org/10.3390/biom10040535.
27. Jade, D. D.; Pandey, R.; Kumar, R.; Gupta, D. Ligand-based pharmacophore modeling of TNF-α to design novel inhibitors using virtual screening and molecular dynamics. *Journal of Biomolecular Structure and Dynamics* **2022**, *40*, 1702-1718, https://doi.org/10.1080/07391102.2020.1831962.
28. Lans, I.; Palacio-Rodríguez, K.; Cavasotto, C. N.; Cossio, P. Flexi-pharma: a molecule-ranking strategy for virtual screening using pharmacophores from ligand-free conformational ensembles. *Journal of Computer Aided Molecular Design* **2022**, *34*, 1063–1077, https://doi.org/10.1007/s10822-020-00329-7.
29. Madzhidov, T. I.; Rakhimbekova, A.; Kutlushuna, A.; Polishchuk, P. Probabilistic approach for virtual screening based on multiple pharmacophores. *Molecules* **2020**, *25*, 385-397, https://doi.org/10.3390/molecules25020385.
30. Maia, E. H. B.; Assis, L. C.; de Oliveira, T. A.; da Silva, A. M.; Taranto, A. G. Structure-based virtual screening: from classical to artificial intelligence. *Frontiers Chemistry* **2020**, *8*, 343, https://doi.org/10.3389/fchem.2020.00343.
31. Schaller, D.; Šribar, D.; Noonan, T.; Deng, L.; Nguyen, T. N.; Pach, S. Next generation 3D pharmacophore modeling. *WIREs Computational Molecular Science* **2020**, *10*, 1468. https://doi.org/10.1002/wcms.1468.
32. Soares Rodrigues, G. C.; Maia, M.; dos, S. A. B.; Costa, B. R. P.; Scotti, L.; Cespedes-Acuña, C. L. Computer-assisted discovery of compounds with insecticidal activity against Musca domestica and Mythimna separata. *Food and Chemical Toxicology* **2021**, *147*, 111899, https://doi.org/10.1016/j.fct.2020.111899.
33. Santana, K.; do Nascimento, L. D.; Lima e Lima, A.; Damasceno, V.; Nahum, C.; Braga, R. C.; Lameira, J. Applications of Virtual Screening in Bioprospecting: Facts, Shifts, and Perspectives to Explore the Chemo-Structural Diversity of Natural Products. *Frontiers Chemistry* **2021**, *9*, 662688, https://doi.org/10.3389/fchem.2021.662688.
34. Ejeh, S.; Uzairu, A.; Shallangwa, G. A.; Abechi, S. E. In silico design, drug-likeness and ADMET properties estimation of some substituted thienopyrimidines as HCV NS3/4A protease inhibitors. *Chemistry Africa* **2021**, *4*, 563-574, https://doi.org/10.1007/s42250-021-00250-y.
35. Ejeh, S.; Uzairu, A.; Shallangwa, G. A. Computational insight to design new potentoial hepatitis C virus NS5B polymerase inhibitors with drug-likeness and pharmacokinetic ADMET parameters predictions. *Future Journal of Pharmaceutical Sciences* **2021**, *7*, 219, https://doi.org/10.1186/s43094-021-00373-6.
36. Hasanshahi, Z.; Hashempour, A.; Ghasabi, F. First report on molecular docking analysis and drug resistance substitutions to approved HCV NS6A and NS5B inhibitors amongst Iranian patients. *BMC Gastroenterology* **2021**, *21*, 443, https://doi.org/10.1186/s12876-021-01988-y.